

A Cyclic Plasticity Model for Multiaxial Behavior of Magnesium

M. Noban¹ and H. Jahed²

¹ University of Waterloo, Waterloo, Ontario, CANADA, mnoban@uwaterloo.ca

² University of Waterloo, Waterloo, Ontario, CANADA, hjahed@uwaterloo.ca

ABSTRACT. *To model the yield asymmetry of magnesium alloys under cyclic tension-compression, the anisotropic directional dependency, and the symmetric behaviour under cyclic pure shear, an anisotropic hardening rule based on Prager-Ziegler hardening model is developed. The proposed model is capable of making explicit reference to shear and axial cyclic material properties in different directions. Hence, the hardening parameter accounts for yield asymmetry and directional anisotropy. The application of the model to the multi-axial loading of AZ61A is carried out. Uniaxial cyclic tension-compression and shear responses of the material is employed to calibrate the material constants in the proposed model. The model is then utilized to predict the stress hysteresis under 90° out-of-phase non-proportional multi-axial loads. Results show very good agreements with the experimental results.*

INTRODUCTION

Environmental and energy concerns has forced transportation sector to seriously consider light weighting of vehicles. In automotive industry, a 10% vehicle mass reduction reduce fuel consumption by 5.7% - 7.4% [1] which in turn reduces greenhouses gas emission by a large factor when considered at a global level. Magnesium (Mg) being the lightest structural metal on earth has shown promises in playing a crucial role in weight saving in transportation and other industries [2]. Currently, Mg consumption in automotive industries is mainly toward non-structural components, and is averaged at close to 5kg per cars manufactured in North America [3]. Further mass reduction should include load-bearing components that are under cyclic loads with variety of load histories including multiaxial loads. Design of fatigue-critical components made of Mg requires cyclic plasticity modeling of this HCP metal.

Among Mg alloys, wrought Mg alloys have high specific strength and are good candidates for load bearing structures. These alloy show a few unusual characteristics that have made their mechanical modeling challenging. Yield asymmetry which is the difference in yield strength in tension and compression, and directional anisotropy [4] are the main characteristics to be considered in any plasticity modeling of Mg alloys. So

far there has been two approaches in developing suitable plasticity models: crystal plasticity methods, and phenomenological continuum methods.

Microstructural methods are based on crystal plasticity that is based on hcp lattice, the deformation mechanisms, texture orientations and other microstructural properties of the material. The two main deformation mechanisms for Mg alloys in room temperature are twinning and basal slip [5]. In addition to basal slip and twinning, pyramidal and prismatic slip systems influence the deformation in specific conditions [6-8]. Interaction between deformations systems, activation of slip mechanisms in different thermal and mechanical conditions and texture orientation are some of the parameters that are considered to develop a constitutive model based on crystal plasticity. These models are implemented in finite element programs [9-10] or as numerical methods, e.g., VPSC model [11-13] and are verified by uniaxial tension and compression tests. However, due to computational complexity these methods are applicable to problems such as uniaxial tension or compression and not yet available for more complex real-life engineering problems.

The second approach, which is traditionally well established and has recently received more attention in modeling Mg, is the phenomenological approach which is the basis of the present research. In this approach, the constitutive models are represented by considering macromechanical behavior of the material independent of micromechanical structure. Phenomenological constitutive models are based on developing a yield criterion and adopting a suitable hardening model. Examples of yield loci are modified von Mises [14], Drucker-Prager [15] and CPB 2006 [16]. Two-Surface plasticity [15] and Frederick-Armstrong [14] and combined Isotropic/Kinematic hardening [16] rules have also been considered as hardening models in order to predict the evolution of yield surface. Similar to crystal plasticity methods, phenomenological constitutive models are often implemented as material models in FE programs such as ABAQUS [14, 16-17] or LS-DYNA [17].

In this paper, an anisotropic hardening rule based on Prager-Ziegler hardening model is developed. The proposed model is capable of making explicit reference to shear and axial cyclic response of material in different directions. Hence, the hardening parameter accounts for yield asymmetry. The application of the model to the multi-axial loading AZ61A [18] is carried out.

BACKGROUND

Figure 1 shows a stable cycle of Mg AZ31B under fully reversed strain-controlled tension-compression test. This figure represents a typical cyclic behavior of wrought Mg alloy in the extrusion direction (c-axis perpendicular to the extrusion axis). Portion 1-2 in Figure 1 is a part of the cyclic curve showing yielding prior to point 2. The deformation mechanism associated with this part is slip as the tension causes contraction along c-axis. The unloading and reverse loading portion 2-3-4 which causes extension along c-axis activates the extension twins and hence yields due to twinning. Twinning causes a rotation of 86° with respect to c-axis as shown by the green

hexagonal prism showing route 3-4 in Figure 1. The unloading from compression, portion 4-5 in Figure 1, show release of twinning strains, detwinning, which makes the curve sigmoidal shape. This will again cause rotation back to untwined stage. The final portion is loading in tension with slip yielding from 5-6.

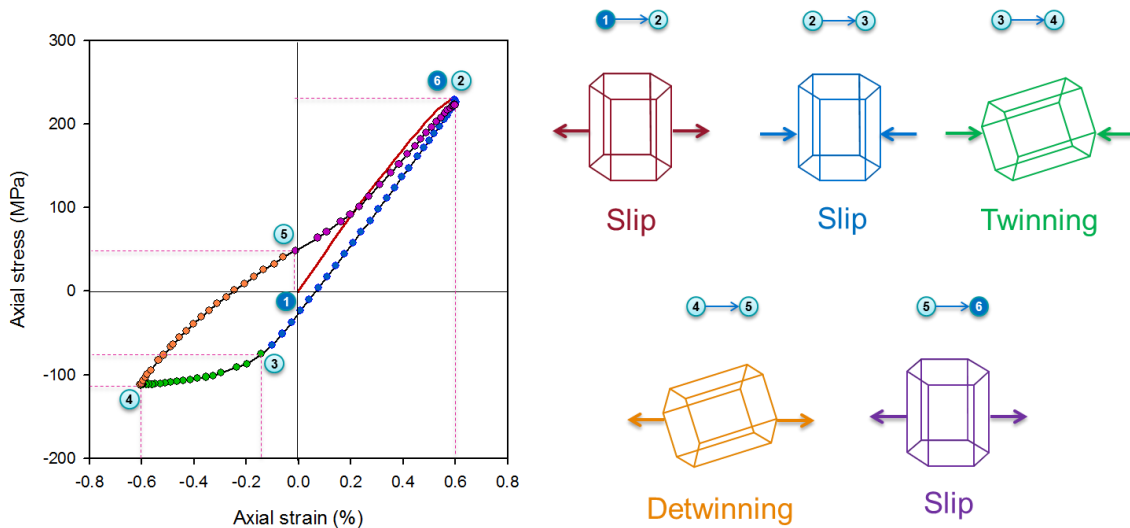


Figure 1: Cyclic behavior of AZ31B at strain amplitude of 0.6% and its corresponding deformation mechanisms [19]

The yield asymmetry in tension and compression is a major characteristic observed from Figure 1. Comparison of points 2 and 3 in the graph shows that yield in compression after unloading from tension is much smaller than yield in tension. It is noteworthy that even the virgin material possesses a different yield in tension than compression. The choice of proper yield function is hence narrowed. The nonmasing effect is another characteristic of the cyclic behavior of wrought Mg alloys. The unsymmetric shape of the hysteresis limits the freedom of adopting a proper hardening rule for modelling this behavior. While the use of isotropic hardening is ruled out due to change in yield in tension and compression, current kinematic hardening rules may also be inadequate because of the change in size of yield surface dictated by the twinning (3-4 in Figure 1) and detwinning (4-5 Figure 1). Moreover, the sigmoidal shape of return reversal (4-6 in Figure 1) requires special treatment.

On the other hand the cyclic shear behavior of wrought Mg alloys is very different from cyclic tension.

Figure 2 shows the cyclic shear behavior of extruded AZ31B in tubular specimens cut along the extrusion direction. Unlike the cyclic tension, the cyclic shear behavior is symmetric and possesses masing effect. A simple Ramberg-Osgood relation can model the cyclic curve and produce hysteresis at different shear strain ranges.

Figure 1and

Figure 2 show behavior in extrusion direction. However, wrought Mg alloys have directional anisotropy.

Figure 3 show the monotonic behavior of AZ31B in extrusion, transverse, and 45° in tension and compression. A cyclic plasticity model for wrought Mg alloy should be able to take into account such anisotropy.

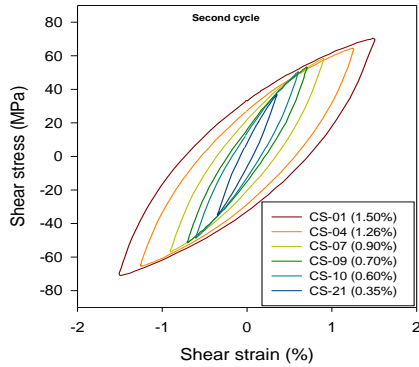


Figure 2: Cyclic shear of AZ31B [3]

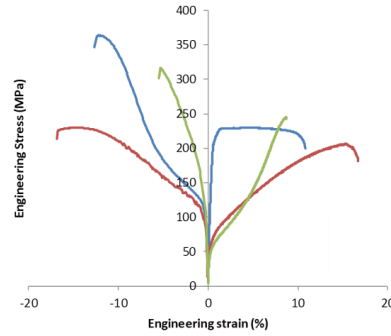


Figure 3: Monotonic behavior of AZ31B extrusion in extrusion direction (blue), transverse direction (green) and 45° (red) [19]

PROPOSED CONSTITUTIVE MODELING

The three major elements of plasticity modelling are the yield function, flow rule, and hardening rule. Yield function defines the onset and subsequent yieldings and dictates when the plasticity calculations need to be followed. It also provides an equivalent measure of mutiaxial stress which assists the material parameter extraction from a simple stress-strain curve. Mises yield function is the most common isotropic yield function and its generalized form in terms of Hill's yield function is applicable to anisotropic materials. More recently, anisotropic yield functions capable of modelling yield asymmetry have been proposed by Cazacu and Barlat [20], and Lee et al [15].

Flow rule builds a constitutive relation between the increment of plastic strain and stress tensors. Most common form is the associated flow rule where the plastic potential is the same as the yield function. A measure of effective plastic strain is usually associated with the flow rule. This measure assist material parameter extraction and also defines the magnitude of the plastic strain tensor.

Hardening rules model the evolution of the yield surface and identify their location in the stress space. There are two general forms of hardening rules known as kinematic hardening and multi-surface models. The first cyclic plasticity model, with the goal of accounting for the Bauschinger effect, was proposed by Prager [21]. Armstrong and Frederick (AF) [22] proposed a nonlinear kinematic hardening model by adding a nonlinear recovery term to Prager's model. Chaboche [23] proposed a model with multiple nonlinear terms to better simulate the hysteresis loop. Another class of cyclic plasticity models, multi-surface, was first proposed by Mroz [24]. Mroz introduced the concept of the field of constant plastic modulus applicable to multiaxial loading conditions. The complexity of multi-surface models lead to the introduction of the two-

surface plasticity model presented by Dafalias and Popov [25] and Krieg [26] to improve computational efficiency.

It has been shown [27] that AF model is capable of defining bounding stress surfaces with different shapes through careful selection of its material parameters. This potentially allows for including the role of an anisotropic yield surface into a hardening rule capable of modeling anisotropy. Hence, the following anisotropic form of Ziegler's hardening rule is proposed,

$$d\tilde{A} = [C] \tilde{m} dp ; \text{ with } \tilde{m} = \frac{\tilde{\sigma} - \tilde{A}}{|\tilde{\sigma} - \tilde{A}|} \quad (1)$$

Where dp and $d\tilde{A}$ are the increments of effective plastic strain and backstress, respectively. Also, $\tilde{\sigma}$ is the stress tensor and \tilde{m} shows the direction of yield surface movement. The $[C]$ matrix in Eq. 1 includes the hardening or plastic moduli. The matrix form of $[C]$ allows for making reference to properties of material in different directions, and hence modeling anisotropic behavior. For example, C_{11} , and C_{22} are defined based on cyclic properties in uniaxial tension-compression in 11 (extrusion) and 22 (transverse) directions while C_{12} depicts the behavior in cyclic shear with respect to 12 direction. With Eq.1 taking care of anisotropy, by considering a low value for initial size of the yield surface one can take any measure of yield function to identify plastic loading. To this effect and to make use of well established Mises associate flow rule, Mises yield and equivalent stress function and associated effective plastic strain is adopted here.

The major task is finding proper forms for the elements of the $[C]$ matrix. Using Eq. 1, the flow rule and the consistency condition (i.e., the stress tensor should always be on the yield surface during plastic loading), the multiaxial plastic moduli is,

$$H_p = \sqrt{\frac{2}{3}} \{n\}^T [C] \{m\} \quad (2)$$

With $\{n\}$ being the normal vector. The multiaxial plastic modulus has the flexibility of being calibrated independently in different directions. The three distinct characteristics of Mg cyclic behavior, yield asymmetry, sigmoidal shape due to twinning and detwinning, and symmetric cyclic shear, discussed in the previous section are now modeled by choosing suitable forms for $[C]$ matrix. To allow yield asymmetry in cyclic tension-compression C_{11} is taken in the following form:

$$C_{11} = C_0 + \sum(\Delta c_{L(i)}) \mu(n_{11}) + \sum(\Delta c_{U(i)}) \mu(-n_{11}) m_{11} \text{ with } \mu(x) = \begin{cases} 0, & x < 0 \\ 1, & x \geq 0 \end{cases} \quad (3)$$

Where L and U refer to loading and unloading, C_0 is the value of plastic modulus right after onset of yielding and assumed to be the same for L and U ; 11 refer to the axial components. For allowing the sigmoidal shape of cyclic tension-compression smooth Heaviside step functions are taken for Δc in the following form,

$$\Delta c_{L(i)} = \frac{h_L(i)}{U(i)} \left(1 + \text{Tanh} \left(\frac{\sigma_{11} - z_{11L}(i)}{d_L(i)} \right) \right) \quad (4)$$

Where h , and d are material constants and z_{11} corresponds to plastic modulus at stress point σ_{11} . Due to the symmetric nature of cyclic shear, Ramberg-Osgood relation is adopted for C_{12} , in the following form with K and n being the material constants for cyclic shear curve:

$$C_{12} = 2^{(1-ns)}(ns) (Ks) \left(\frac{2^{(ns-1)}s}{Ks} \right)^{\frac{ns-1}{ns}} (\sqrt{2} m_{12}); \text{ with } s = |\max(\sigma_{12})| + \text{Sign}(n_{12})\sigma_{12} \quad (5)$$

APPLICATIONS TO MODELING CYCLIC BEHAVIOR OF AZ61

The model is applied to cyclic behavior of AZ61 [18]. To be able to incorporate the effect of the strain amplitude, ϵ_a , on the material constants, an axial strain memory parameter, ϵ_a , is employed. Using the uniaxial cyclic tension-compression and cyclic shear at different strain amplitudes, the calibration constants in Eq. 4 and 5 were found and are reported in tables 1. It was found that Eq. 4 would be best fitted to data by using a two-term function for loading and one-term function for unloading.

Table 1: Material constants for AZ61

AZ61	First term	Second term
$z_{11L}(i)$	-70	$3.4 \times 10^4 \epsilon_a^2 + 22802 \epsilon_a - 129.33$
$h_L(i)$	-294300	$2.39 \times 10^9 \epsilon_a^2 - 4.5 \times 10^7 \epsilon_a + 224413$
$d_L(i)$	40	20
$z_{11U}(i)$	$-1.683 \epsilon_a^2 + 32320 \epsilon_a - 120.9$	0
$h_U(i)$	-311100	0
$d_U(i)$	90	0
Shear	K= 297 MPa, n=0.267	

Figure 4 shows the uniaxial cyclic curves reproduced using the proposed model as compared to experimental results. The comparison is over a wide range of strain amplitude, from 0.3% to 0.9%, and the predictions are in good agreement with the experimental results. Note that the mean stress and the maximum and minimum stress responses in tension-compression that shows yield asymmetry are well predicted by the model. The shear strain amplitudes are also over a wide range covering strain values from 0.57% up to 1.6%, with very good agreement between prediction and experimental results.

With the calibration constants obtained from uniaxial curves, the multiaxial stress-strain response of AZ61 under out-of-phase loading was predicted by the model. Figure

5 shows the prediction results compared to experiment. Both axial and shear responses predicted by the model are in good agreement with the experimental results.

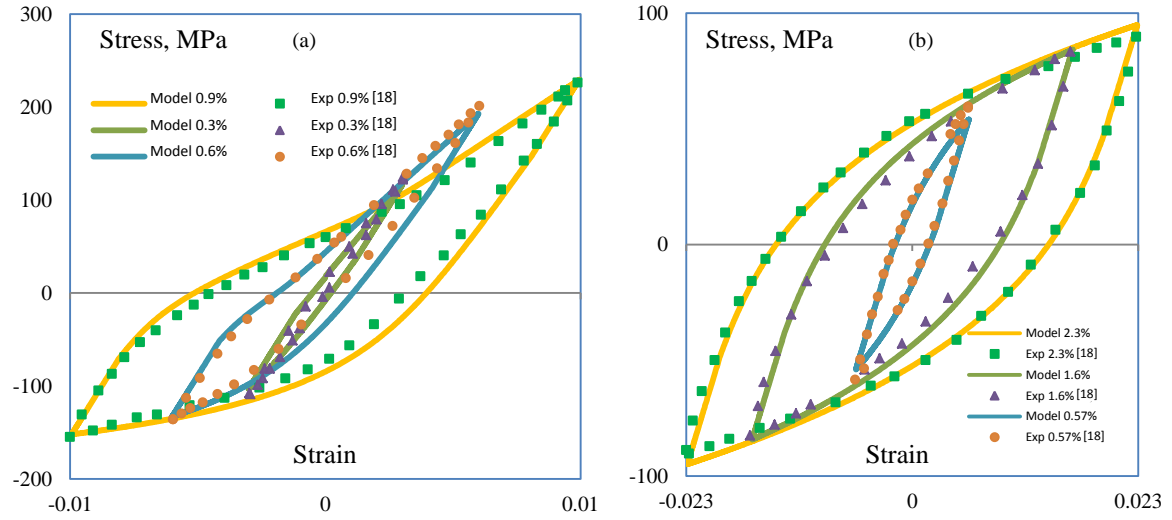


Figure 4: Model prediction and experimental results; (a) tension-compression; (b) shear

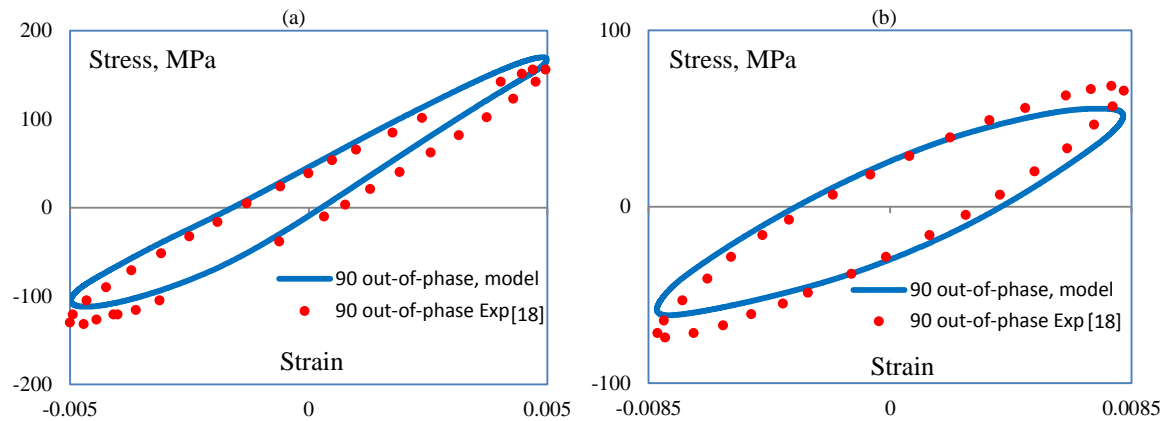


Figure 5: Model prediction and experimental results for hysteresis under 90° out-of-phase loading for $\epsilon_a = 0.5\%$, $\gamma_a = 0.8\%$; (a) axial stress-strain response; (b) shear stress-strain response

CONCLUSIONS

An anisotropic cyclic plasticity model based on modified Ziegler hardening model capable of modeling yield asymmetry is proposed. The modification entails a matrix format of the hardening modulus. Material behaviour in different directions is present in the matrix containing the hardening modulus parameter. The material constants in the model are calibrated using material response under cyclic axial and shear loadings. A Heaviside step function for axial loading and Ramberg-Osgood power law function in shear loading has been employed for calibrating the model. It is shown that the model is

able to produce sigmoid shape and asymmetric hysteresis loops in axial direction, and symmetric hysteresis loop in shear direction. The model is employed to predict the cyclic tension-compression, torsion and multiaxial behaviour of magnesium alloy AZ61. The model's predictions are found to be in good agreements with experimental observations.

REFERENCES

1. National Research Council. (2011) Academies Press, Washington DC.
2. B. Davis, (2012) *9th international conference on magnesium alloys*, Vancouver.
3. J. Albinmoussa J, H. Jahed H, S. Lambert. (2011) *Int J Fatigue*, **33**(11):1403, 1416.
4. Ball, E., & Prangnell, P. (1994) *Scripta Metallurgica et Materialia*, **31**(2), 111-116.
5. Klimanek P., Potzsch A. (2002). *Materials Sci and Eng*, A324, 145–150.
6. Schmid, E., & Boas, W. (1935) *Plasticity of Crystals*. Chapman & Hall, London.
7. Ward-Flynn, P., Mote, J., & Dorn, J. (1961) *Transactions of the Metallurgical Society of AIME*, **221**, 1148-1154.
8. Ando, S., & Tonda, H. (2000) *Materials Science Forum*, 350-351, 43-48.
9. Staroselsky, A., & Anand, L. (2003). *Inte J of Plasticity*, **19**, 1843-1864.
10. Fernández, A., Pérez Prado, M., Wei, Y., & Jérusalem, A. (2011) *Int J of Plasticity*, **27**, 1739-1757.
11. Proust, G., Tomé, C., Jain, A., & Agnew, S. (2009) *Int J of Plasticity*, **25**, 861-880.
12. Jain, A., & Agnew, S. (2007) *Materials Sci and Eng*, A462, 29-36.
13. Lévesque, J., Inal, K., Neale, K., & Mishra, R. (2010) *Int J of Plasticity*, **26**, 65-83.
14. Li, M., Lou, X., Kim, J., & Wagoner, R. (2010) *Int J of Plasticity*, **26**, 820-858.
15. Lee, M.-G., Wagoner, R., Lee, J., Chung, K., & Kim, H. (2008) *Int J of Plasticity*, **24**, 545-582.
16. Kim, J., Ryou, H., Kim, D., Kim, D., Lee, W., Hong, S.-H., et al. (2008) *Int J of Mech Sci*, **50**, 1510-1518.
17. Oberhofer, G., Dell, H., Gese, H., Dr. Lanzerath, H., Wesemann, J., & Hombergsmeier, E. (2003) *4th European LS-DYNA Users Conference*.
18. J. Zhang, Q. Yu, Y. Jiang and Q. Li, (2011) *Int. J. Plasticity*, **27**(5):768-787,
19. J. Albinmoussa (2012), PhD Thesis, University of Waterloo, Canada.
20. Cazacu O., Barlat F. (2004) *Int J Plasticity*, **20**:2027–2045,
21. Prager W. (1956) *J Applied Mechanics*, **23**:493-496,.
22. Armstrong P, Frederick. (1966) C.CEGB report RD/B/N731, Berkeley Nucl. Laboratory.
23. Chaboche JL, Rousselier. (1983) G. *ASME J. Pressure Vessel Technol*, **105**:153-158.
24. Mroz Z. J. (1967) *Mechanics and Physics of Solids*,**15**:163–175.
25. Dafalias Y, Popove, E. (1971) *ASME J Applied Mechanic*, **9**:645–651.
26. Krieg R. (1975) *ASME J Applied Mechanics*, **42**:641–646.
27. Jiang Y, and Kurath K. (1996) Characteristics of the Armstrong-Frederick type plasticity models. *Int. J. Plasticity*, **12**:387-415.